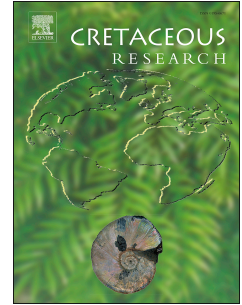


Accepted Manuscript

Unusual soft tissue preservation in the Early Cretaceous (Aptian) crocodile cf. *Susisuchus* from the Crato Formation of north east Brazil

Grant J. Field, David M. Martill



PII: S0195-6671(16)30326-3

DOI: [10.1016/j.cretres.2017.04.001](https://doi.org/10.1016/j.cretres.2017.04.001)

Reference: YCRES 3577

To appear in: *Cretaceous Research*

Received Date: 8 November 2016

Revised Date: 2 April 2017

Accepted Date: 2 April 2017

Please cite this article as: Field, G.J., Martill, D.M., Unusual soft tissue preservation in the Early Cretaceous (Aptian) crocodile cf. *Susisuchus* from the Crato Formation of north east Brazil, *Cretaceous Research* (2017), doi: 10.1016/j.cretres.2017.04.001.

This is a PDF file of an unedited manuscript that has been accepted for publication. As a service to our customers we are providing this early version of the manuscript. The manuscript will undergo copyediting, typesetting, and review of the resulting proof before it is published in its final form. Please note that during the production process errors may be discovered which could affect the content, and all legal disclaimers that apply to the journal pertain.

1 Unusual soft tissue preservation in the Early Cretaceous
2 (Aptian) crocodile cf. *Susisuchus* from the Crato Formation of
3 north east Brazil

4
5 Grant J. Field, David M. Martill

6
7 *School of Earth and Environmental Sciences, University of Portsmouth, Portsmouth, PO1 3QL, UK*

8
9 ABSTRACT

10
11 A new specimen of the neosuchian crocodylomorph, *Susisuchus* sp. from the Lower
12 Cretaceous (Aptian) Crato Formation of Ceará, North East Brazil is remarkable for extensive
13 preservation of the epidermis and limb musculature. The specimen comprises incomplete
14 post-cranial remains, including an articulated sequence of thirteen thoracic vertebrae, a
15 disarticulated pair of lumbar vertebrae and all four limbs articulated in varying degrees of
16 completeness but divorced from the axial skeleton. Soft tissues are preserved in two distinct
17 modes, in close association with the skeletal remains. An external mould of the dorsolateral
18 scales of the trunk extends over a bedding plane surface while mineralisation of soft tissues
19 preserving the musculature surrounds the left forelimb. Soft tissue preservation is extremely
20 rare in crocodylomorphs and this is only the second report of soft tissue preservation in a
21 crocodylian from the Crato Formation.

22
23 *Keywords:*

24 Crato Formation
25 Cretaceous
26 Crocodylomorpha
27 Neosuchia
28 *Susisuchus*
29 Soft tissue preservation
30
31

32 **1. Introduction**

33 A new specimen (UERJ-PMB R07) comprising the partial skeleton of a susisuchid
34 crocodylian from the Crato Formation of north east Brazil is remarkable for the extensive soft
35 tissue preservation intimately associated with the skeletal remains. Crocodylian remains are
36 extremely rare in the Crato Formation (Salisbury et al., 2003, Frey and Salisbury, 2007,
37 Figueredo and Kellner, 2009, Figueredo et al., 2011), which is otherwise better known for the
38 abundance of its invertebrates (primarily insects, but also arachnids and decapod crustaceans
39 (Bechly, 2007, Dunlop et al., 2007, Schweigert et al., 2007 respectively)). Vertebrates in the
40 Crato Formation are diverse, including osteichthyans (Brito, 2007), amphibians (Baéz et al.,
41 2009), turtles (Naish, 2007), lizards (Martill, 2007), pterosaurs (Unwin and Martill, 2007) and
42 an ancestral snake (Martill et al., 2015). A wide variety of flora are also preserved including
43 many early angiosperms (Mohr et al., 2007).

44 Soft tissue preservation has previously been reported in Crato Formation vertebrates,
45 having been described for the head crests and wing membranes of the pterosaurs *Tapejara*
46 (Frey et al., 2003a, b) and *Tupandactylus* (Kellner and Campos, 2007) and the limbs of the
47 turtle *Araripemys* (Fielding et al., 2005). Soft tissues were found in the holotype of the

48 neosuchian crocodile *Susisuchus anatoceps* as amorphous goethite stains, a result of
49 weathering of low-fidelity mineralisation most likely by iron sulphides (Salisbury et al.,
50 2003). Here we describe another example of cf. *Susisuchus* sp., in which soft tissues are
51 preserved associated with the thoracic and appendicular skeleton. For a more detailed account
52 of the palaeontology of the Crato Formation the reader is referred to Martill et al. (2007).

53

54 *Abbreviations used*

55 The specimen described here is deposited in the collection of the Departamento do
56 Zoologia of the Universidade Estadual de Rio de Janeiro, R.J., Brazil, accession number
57 UERJ-PMB R07. SMNK; Staatliches Museum für Naturkunde Karlsruhe, Karlsruhe,
58 Germany. UFRGS; Laboratory of Vertebrate Palaeontology, Universidade Federal do Rio
59 Grande do Sul, Porto Alegre, RGS, Brazil.

60

61 **2. Locality and Geology**

62 *2.1 Locality*

63 The new specimen was obtained by one of the authors (DMM) while on field work in
64 the Araripe Basin in 2006. It was given by a quarry worker, who was digging limestone
65 between the small towns of Nova Olinda and Santana do Cariri in the South of Ceará, north
66 east Brazil. This area has been extensively exploited for laminated limestone and has proven
67 to be one of the most productive sites worldwide for Lower Cretaceous non-marine fossils.
68 The stone quarries are located on the flanks of the Chapada do Araripe, a large tableland
69 dominated by Upper Cretaceous strata (Fig. 1 and 2). It outcrops around the Chapada do
70 Araripe in both southern Ceará and Pernambuco, with possible equivalents in Piauí. It is

71 missing in some places due to overlapping by younger strata. The formation can be traced
72 extensively around the chapada, but is only excavated for paving stone in the area between
73 Tatajuba, Santana do Cariri and Nova Olinda, and at one site near the town of Crato, but the
74 vast majority of fossils are found in the Nova Olinda-Santana do Cariri region of Ceará. A
75 large excavation in the Crato Formation at Barbalha for cement production does not yield
76 abundant fossils.

77 **(Fig. 1. Locality map)**

78

79 *2.2 Geological Setting and Stratigraphy*

80 The Crato Formation is a heterolithic clastic/carbonate sequence of lacustrine,
81 lagoonal and possibly deltaic facies. Extensive and labour intensive, manual quarrying of the
82 Nova Olinda Member limestone at the base of the formation results in very many fossils
83 collected by the quarrymen. Ever since the late 1980s these numerous quarries have been the
84 source of many spectacular fossils (for a summary see Martill et al., 2007). These strata are
85 dated as late Aptian by Batten (2007) on the basis of the palynoflora. For details on the
86 stratigraphy of this unit and its areal extent see Martill and Heimhofer (2007).

87 The Crato Formation rests either unconformably on Neoproterozoic basement or
88 conformably on strata of the Batateiras Formation (names vary depending on authors, e.g.
89 Missao Velha Formation of Beurlen, 1962). Where it sits with stratigraphic conformity on
90 older strata there appears to be a transition from mudstones and siltstones of the Batateiras
91 Formation into laminated limestones. Such conformable sequences are best seen in the region
92 around the town of Crato and near Nova Olinda. In many places, however, a topographic
93 unconformity is present, representing a submerged palaeo-landscape of some considerable
94 relief. This ancient terrain is composed of low grade metamorphic rocks with granitic

95 intrusions and coarse, immature sandstones of the Cariri Formation that may have
96 represented islands within the Crato Formation lagoon/lake system (Martill and Heimhofer,
97 2007).

98 The fossiliferous, laminated limestones of the Nova Olinda Member that form the
99 fossil Lagerstätte are well exposed around Nova Olinda in many quarries and natural bluffs.
100 It is also quarried near Crato, but elsewhere, although well developed, the limestones appear
101 to be largely devoid of fossils.

102 **(Fig. 2. Strat log)**

103

104 **3. Materials and Methods**

105 *3.1 Material*

106 The new specimen, preserved on a typical (for the Nova Olinda Member) slab of
107 cream coloured, laminated limestone has contrasting preservational styles (Fig. 3 and 4). The
108 slab has a sub-triangular outline, with the specimen extending over the majority of its surface.
109 Numerous pellet-like structures are scattered over the bedding plane surface, which is also
110 typical, and distinctive for this unit. The specimen is remarkable for the exquisite
111 preservation of epidermal scales of the body flank and dorsal surface as well as an intriguing
112 preservation of soft tissues of the limbs. The scales of the trunk have been preserved as a soft
113 tissue impression while the soft tissues of the right forelimb have been mineralised. Material
114 similar to that around the right forelimb is preserved around the left femur however much of
115 it appears to have been removed during preparation in the quarry with little material
116 remaining. The epidermal scales are not, as might be supposed, moulds of the inferior surface
117 of osteoderms, as in places overlapping sediment shows no bone material between the
118 overlying and underlying lamina.

119 There are just two osteoderms preserved, both detached from the body. One displays
120 its upper surface of small pits, while the other its lower surface which is smooth. All four
121 limbs are preserved, with the forelimbs articulated and nearly complete with both manus. The
122 hind limbs are less complete but include the femur, tibia and fibula, as well as fragments of
123 the pelvis in the left hind limb. The right hind limb includes the tibia, fibula, metatarsals and
124 disarticulated elements of the pes. The appendicular skeleton is detached from the axial
125 skeleton however remains close to life position. The vertebral column is articulated for a
126 length of thirteen thoracic vertebrae exposed in ventral view. There are two detached lumbar
127 vertebrae lying to one side at the posterior end of the sequence.

128 There has been damage to the specimen caused by splitting of the slab during the
129 excavation and in preparation, which has been poorly repaired with what appears to be an
130 adhesive past. A gritty material has been used to fill in some damaged areas of the specimen
131 and slab on both sides and several chisel marks have damaged part of the exposed soft tissues
132 of the trunk. Some bones have been repaired and glued into place as they appear to have
133 dropped from the slab during preparation.

134

135 *3.2 Methods*

136 The specimen has been examined under UV light and by light and scanning electron
137 microscopy. No additional preparation was performed on the specimen in order not to further
138 damage the surface with soft tissues, but small samples of the soft tissue of the forelimb were
139 removed for analysis by scanning electron microscopy and energy dispersive x-ray
140 spectroscopy. Samples examined by electron microscopy were mounted on flat aluminium
141 stubs, sputter coated with a gold-palladium alloy and examined using a JEOL JSM 6100

142 machine. The specimen was photographed using an Olympus E-420 DSLR camera and
143 images were processed using Adobe Photoshop CC 2015.

144 **(Fig. 3. Specimen photo)**

145 **(Fig. 4. Schematic)**

146

147 **4. Description**

148 *4.1 Systematic Palaeontology*

149 Crocodyliformes Hay, 1930

150 Mesoeucrocodylia Whetstone and Whybrow, 1983

151 Neosuchia Benton and Clark, 1988

152 Susisuchidae Salisbury et al., 2003

153 cf. *Susisuchus* Salisbury et al., 2003

154 Specimen: Partial skeleton of a neosuchian including axial and appendicular elements of both
155 girdles and areas of extensive soft tissue preservation referred to cf. *Susisuchus* sp. Accession
156 number UERJ-PMB R07 (Universidade do Estado do Rio de Janeiro).

157 UERJ-PMB R07 is identified as a crocodyliform due to the presence of typical
158 crocodylian osteoderms with smooth basal surface and pitted epidermal surface shown, and a
159 crocodylian type squamation of the trunk integument. The amphicoelous vertebrae show that
160 it belongs in Mesoeucrocodylia. The clade Neosuchia is diagnosed on cranial features and
161 features of the neural spines (Benton and Clarke, 1988), both elements that are not visible in
162 the specimen. A neosuchian affinity is assumed based on its identification and hinted at by

163 the neosuchian-like proportions of the limbs with a forelimb-hind limb ratio of approximately
164 0.85.

165 Its familial placement within Susisuchidae is based upon the same features used to
166 diagnose the specimen as cf. *Susisuchus*. In comparing the specimen with the two crocodylian
167 genera reportedly previously from the Crato Formation by Salisbury et al. (2003) and Frey
168 and Salisbury (2007) UERJ-PMB R07 appears closer to *Susisuchus* than *Araripesuchus*. Both
169 taxa are diagnosed primarily on cranial features not visible in the specimen. Nevertheless,
170 other diagnostic features are present in the forelimbs of UERJ-PMB R07; the presence of
171 unguals only on manual digits I and II, and the maximum width of the proximal extremity of
172 the ulna is approximately twice the minimum width of the ulna shaft, the distal extremity
173 cannot be confidently compared due to damage. Furthermore, the limb proportions of UERJ-
174 PMB R07 are more closely allied to those of *Susisuchus* and so we here refer the specimen to
175 cf. *Susisuchus* sp. A palaeohistological study on *Susisuchus* has identified the animal as a
176 dwarf taxon, markedly smaller than other crocodylomorphs from the Cretaceous (Sayão et
177 al., 2016), and consequently the new specimen is considered a sub-adult due to its size.

178

179 *4.2 Description*

180 *Axial skeleton*

181 *Lumbar vertebrae.* Two lumbar vertebrae are articulated and preserved in ventral view (Fig.
182 5), detached from the axial skeleton but still in close association with the thoracic vertebrae.
183 One lumbar vertebra is preserved as a broad, flat shelf, the transverse processes extending
184 from the ventral surface of the centrum and broadening distally with an aspect ratio of 24:9
185 for the total width: length. The second lumbar vertebra appears more typical of other centra
186 however matrix exposure obscures other details.

187

188 *Thoracic vertebrae.* An articulate sequence of thirteen thoracic vertebrae are preserved,
189 exposed in ventral view. These are considered thoracic vertebrae based on their position
190 relative to the limbs of the animal and the presence of articular facets for the ribs present on
191 the anterior edge of the transverse processes of several vertebrae. The centra of the eight
192 posterior-most thoracic vertebrae are preserved but the ninth centrum has been damaged,
193 lacking the anterior half. The centra of the four anterior vertebrae are not present, likely in the
194 missing counter slab, exposing the mineralised neural canal parallel to the bedding surface.

195 Several of the posterior thoracic vertebrae are damaged revealing detail of the
196 articular surfaces. They are amphicoelous indicating mesoeucrocodylian affinities (Frey
197 and Salisbury, 2007). The transverse processes become shorter and thinner towards the
198 cranial end of the preserved sequence. Further anterior vertebrae may be preserved in the
199 sequence but preserved on the counter slab.

200 **(Fig. 5. Vertebrae photo and schematic)**

201

202 *Appendicular skeleton*

203 *Pectoral girdle.* A thin, sheet-like fragment of bone overlies the proximal right humerus and
204 is considered to be part of the pectoral girdle. Although it lacks landmarks and cannot be
205 confidently identified, it is likely a portion of the right scapula due to the arrangement of the
206 bones. Other fragments of bone are also present between the forelimbs but are similarly
207 unidentifiable and may be part of the proximal right humerus, the pectoral girdle or
208 osteoderms.

209 *Forelimb*

210 *Humerus*. Both humeri are preserved and exposed in posterior view (Fig. 6). They are almost
211 complete missing just the proximal end in the left humerus, which is damaged and is
212 obscured by matrix. Despite fragments of the pectoral girdle obscuring much of the proximal
213 third of the right humerus, the point at which it terminates appears visible before it extends
214 beneath the soft tissue impressions. Using the visible range, the humerus measures at 45 mm,
215 here used as an approximate total length for the humerus.

216 The corpus is slender, smooth and round in cross-section with a diameter of 4 mm,
217 roughly one third the width of the distal end. In the right forelimb, where much of the corpus
218 is broken and absent, a cross-section reveals the interior of the bone and a mineral filled
219 medullar cavity. The distal end of the humerus appears typical of *Susisuchus anatoceps* with
220 two distinct ridges on the medial and lateral side extending from both distal condyles
221 (Salisbury et al. 2003), more pronounced in the left humerus than in the right. These extend
222 for 12.5 mm, approximately one quarter the length of the humerus, forming a concave facies.

223

224 *Ulna*. Both ulnae are damaged due to prior preparation with the right ulna lacking its distal
225 third and a section of the proximal corpus, but an impression of the bone remains. The corpus
226 of the right ulna has been broken off and glued back in place but appears displaced at the
227 distal end. The proximodistal length of the right ulna is 29 mm, with an ulna-humeral ratio of
228 0.66 and a corpus minimum width of 2mm. Both the proximal and distal ends are broad
229 compared to the shaft, the proximal being the broader end twice the width of the corpus, the
230 distal extremity damaged but similar in width. Both heads have convex facies but are
231 otherwise featureless.

232

233 *Radius.* As with the ulnae the radii have been damaged. The distal end of the right radius has
234 broken off and been glued back into place, deep scratches extend along the length of the
235 corpus. Similar to the right humerus, a broken cross-section exposes the mineral filled
236 medullar cavity and the solid nature of the bone wall. In the left radius the corpus has been
237 broken off and glued back into place, a gritty material has been added to the glue around the
238 distal end displacing the bone.

239 The radius is slightly shorter than the respective ulna, approximately 95% its
240 proximodistal length but the corpus is also 2mm thick. Both heads are smaller than in the
241 ulna, the distal head 2mm thick and the proximal 4mm thick. The articular ends of both radii
242 are flat and the proximal end of the left radius is inflected dorsally. This is not present in the
243 right radius and may be an artefact of damage to the rock, where it has been repaired, or to
244 the bone where it has been broken and glued.

245
246 *Carpals.* Both the radiale and ulnare are preserved in the right forelimb but are absent in the
247 left. Both are small elements, the radiale measuring 7.5 mm in length, the ulnare measures 5
248 mm in length. The radiale is a flat, hourglass-shaped element with a minimum thickness of
249 1.5 mm. The proximal end is wider than the distal end at 3.5 mm compared to 3 mm. The
250 ulnare is also hourglass-shaped with a less pronounced distal end, just 1.5 mm wide
251 compared to the minimum width of 1 mm and the proximal end measuring 2.5 mm wide.

252
253 *Manus.* Both manus are preserved in association with their respective limbs and are largely
254 articulated and almost complete but the left manus is detached from the forelimb but still
255 closely associated with it. In the left manus, metacarpals II-V are present, and in the right
256 metacarpals I-III and V are present. Metacarpal IV may also be present in the right manus but

257 is obscured by sediment and other metacarpals and so cannot be confidently described as
258 either a metacarpal or a phalanx. The metacarpals are typically long and slender with lengths
259 of 3.5 mm to 8 mm and thicknesses of 0.5 – 1.5 mm. Metacarpal I is both the shortest and
260 thickest metacarpal.

261 In the right manus all digits are preserved but in varying completeness. Digits I and II
262 are the only two complete digits comprising of two and three elements respectively. The
263 ungual of digit I is a blunt, thick element compared to the other unguals with a very gentle
264 curvature whereas digit II's ungual is partially obscured by sediment. Digit III comprises
265 three phalanges but lacks an ungual as is diagnostic of *Susisuchus*. Digit IV consists of two
266 medial phalanges adjacent to digit III, digit V is preserved as phalanx 1 and a mould of
267 phalanx 2. In the left manus digits I-III and V are preserved but no elements from digit IV are
268 identified. Both phalanges are again preserved of digit I, however phalanx 1 is preserved only
269 as the distal portion. Three phalanges are preserved in digit II with a less obscured view of
270 the ungual, which is more strongly curved than in digit I and is significantly sharper. Three
271 phalanges are preserved in digit III and two from digit V.

272 **(Fig. 6. Forelimb photo and schematic)**

273

274 *Pelvic girdle.* A broken piece of sheet-like bone is preserved adjacent to the right femur,
275 pressed against the proximal end. It is considered to most likely be a portion of the pubis
276 based on the general morphology but it lacks useful landmarks as is typical of the cranial end
277 of the pubis. A cross-section of bone is visible in an adjacent surface of the rock and is likely
278 a fragment of the ischium, but it cannot be confidently identified.

279

280 *Hind limb*

281 *Femur.* The left femur is preserved and is complete in length however the proximal end is
282 both obscured in part by a fragment of the pelvic girdle and has been damaged, the femoral
283 head split along the bedding plane. It appears to still be in association with the pubis. The
284 femur is similar in length to the humerus, measuring slightly shorter proximodistally at 44.5
285 mm long. The corpus is smooth and round in cross-section and as thick as the humeral corpus
286 at 4 mm, but is curved posteriorly. The distal end is broad, almost three times the thickness of
287 the corpus, with distinct medial and lateral ridges extending for 11 mm.

288
289 *Tibia.* The tibia is a long, straight bone, approximately 90% the proximodistal length of the
290 femur at 39.5 mm long. It is preserved in both limbs but is significantly damaged in the right
291 hind limb, the proximal third having been broken off and repaired. The corpus is slender a 2.5
292 mm thick with a broad, robust and curved proximal head and a broad, flat distal head, both
293 almost three times as wide as the corpus is thick. The surface is smooth except for at the
294 proximal head of the right tibia where striations extend lengthways, parts of the head have a
295 fibrous texture, however, this may be a result of degradation. Damage at the distal end of the
296 left tibia reveals a hollow interior.

297
298 *Fibula.* The fibula is present in both hind limbs, complete in the left, although the distal end
299 is damaged where the rock has been cut, and heavily damaged along the corpus in the right,
300 the distal head broken off lying adjacent to the corpus. The fibula is slightly shorter than the
301 tibia at 39 mm long and is slender, the corpus 2 mm thick and the distal head 4 mm thick. The
302 proximal head is obscured by the tibia in the left hind limb but is visible in the right
303 measuring 2.5 mm thick.

304

305 *Tarsals.* Tarsals are only preserved in the right hind limb. They are small, smooth, round
306 bones, the lateral tarsal is the smaller of the two. The medial tarsal is a rounded square bone,
307 7.5 mm long and 5 mm thick. The lateral tarsal is semi-circular with a flattened lateral face,
308 only 4.5 mm long and 3 mm thick.

309

310 *Metatarsals and pes.* Three metatarsals are preserved in the right hind limb. They are long,
311 slender bones, all measuring at least 22 mm in length and between 1.5 mm and 2 mm thick.
312 The proximal end is very broad in metatarsal I, three times as thick as the corpus and twice as
313 thick as metatarsal III, the proximal head of metatarsal II obscured by metatarsal I. The distal
314 ends of metatarsal II and III are damaged and incomplete while metatarsal I has a broad distal
315 end, 4 mm wide, with a pit in the centre of the head. Damage to metatarsal III at the distal
316 end reveals a cavity. Phalanges from the right pes are preserved but disarticulated and
317 overlapping each other at the distal end of the metatarsals. A single ungual is identifiable
318 disassociated from the pes, it is a heavily curved, sharp bone 7 mm in length.

319 **(Fig. 7. Hind limbs photo and schematic)**

320

321 *Osteodermal skeleton*

322 Two osteoderms are identified in association with the specimen, one located near the
323 left hind limb but is relatively distant from other skeletal elements except for unidentifiable
324 bone fragments, potentially other osteoderms. This osteoderm has a rounded margin as well
325 as typically crocodylian pitting of the dorsal surface. The rounded margin suggests that this
326 osteoderm was probably an accessory osteoderm of the dorsal body shield (Salisbury et al.,
327 2003). The osteoderm appears to be broken during preparation.

328 A second osteoderm is located adjacent to the distal left humerus and is exposed in
329 ventral view. It is identified as an osteoderm despite the unfavourable view based upon the
330 uneven margin consistent with the pitting of osteoderms. The surface exposed is smooth and
331 rectangular in shape, however, the osteoderm may extend further beneath the humerus too. It
332 cannot be confidently identified based upon the lack of landmarks present on the ventral
333 view.

334

335 **5. Results**

336 *5.1 Light microscopy*

337 Microscopic analysis was utilised to examine the enigmatic nature of the soft tissues
338 surrounding the right forelimb. The material is a mixture of rounded to sub-angular grains
339 ranging from 0.5 mm to 2.0 mm in diameter. Microscopic analysis of this mineralised
340 material alleviated concerns that it may have been an artificial cement, these concerns were
341 disproved by the relationship of the grains with the skeletal elements and the surrounding
342 limestone. The mineralogy is seen growing around the skeletal elements, around both sides
343 and underneath, where the humeral corpus and the distal corpus and head of the ulna is
344 missing the same granular mineralogy is observed on the underside (Fig. 8A). Individual
345 grains are also observed grown into the surrounding rock (Fig. 8B). The grains appear to
346 consist of calcite, silicified material and fragments of bone. The granular material is a mix of
347 brown, orange and black grains of calcite and grey siliceous grains.

348 **(Fig. 8 Microscopy photos)**

349 *5.2 SEM Analysis*

350 An SEM analysis was carried out on the mineralogy of the soft tissues surrounding
351 the right forelimb. The grains analysed were a mixture of rounded grains and irregularly
352 shaped grains (Fig. 9). All of the grains studied appear to have a similar structure despite
353 variation in shape. The surface of the grains is typically smooth and undulating forming a
354 shell-like structure, some of these surfaces also include small holes only a few micrometres
355 across covering the surface (Fig. 9). Orthogenic calcite crystals are also noted, growing on
356 these grains (Fig. 9).

357 **(Fig. 9 SEM plate)**

358 *5.3 EDX spectrometry*

359 Further compositional analysis was carried out using EDX spectrometry. The
360 specimen was prepared using a gold-palladium coating and as such associated peaks are
361 ignored in readings. The primary composition of the sample was found to be calcium, carbon,
362 oxygen and iron (Fig. 10A, B), attributed to calcite and iron oxides. Silicon is identified as
363 the next most common element, likely a result of the silicification noted around some areas of
364 the slab, including around several elements of the fossil. Other elements found in smaller
365 quantities include manganese, zinc, chlorine, barium, lead, potassium and copper (Fig. 10C,
366 D), all associated with other minerals found at lower strata within the Crato Formation.

367 **(Fig. 10 EDX spectrometry)**

368 *5.4 Ultra-Violet Imaging*

369 Ultra-violet imaging of the specimen was undertaken to aid in the identification and
370 observation of skeletal elements and to identify if any mineralised tissues were present in
371 association with the soft tissue impressions of the trunk. Skeletal elements fluoresced under
372 ultra-violet lights, allowing easier analysis of elements difficult to observe under normal
373 lighting (Fig. 11A, B). The soft tissue impressions however, did not fluoresce, nor did the

374 mineralised material around the right forelimb (Fig. 11B). The similar mineralised material
375 around the right hind limb does fluoresce however (Fig. 11A). Silicified sediment fluoresced
376 around the right manus, closely following the soft tissue outline, and in the area surrounding
377 the right hind limb.

378 **(Fig. 11 UV images)**

379

380 **6. Taphonomy**

381 *6.1 Preservation*

382 All of the skeletal elements present in the specimen are preserved as three-
383 dimensional brown biominerals. Elements are situated relatively parallel to the bedding plane
384 except for the proximal and distal vertebral elements, which penetrate into the sediment. The
385 preserved bones are typically smooth and solid with the exception of the right tibia and fibula
386 in which the proximal and distal heads have a fibrous texture. Where the femoral head has
387 been damaged in the right hind limb, the interior appears crystalline with dendrites inside the
388 bone. Where the humerus and radius of the left forelimb are damaged, however, the bone
389 appears consistent with the exterior with a mineralised medullar cavity. The neural canal of
390 the anterior thoracic vertebrae appears to have been infilled with calcium carbonate and is
391 slightly more orange than the surrounding limestone.

392 Soft tissue preservation is reported in two modes in this specimen. An impression of
393 the dorsolateral integument of the trunk has been preserved on a bedding plane extending
394 from around the eighth preserved thoracic vertebra to the left forelimb (Fig. 3 and 12). The
395 impression shows detail of the specimen's scale arrangement. Ultra-violet imaging reveals
396 that there are no traces of mineralised soft tissues in association with the integument. The
397 other form of soft tissue preservation, unique to this specimen in the Crato Formation, is the

398 enigmatic mineralised material surrounding the right forelimb from the proximal head of the
399 humerus to the wrist (Fig. 3 and 6). Similar mineralisation is observed around the femur of
400 the right hind limb but notably less is preserved, largely as orange-brown staining, possibly
401 removed during preparation (Fig. 7). The mineralogy is described as primarily calcium
402 carbonate (Fig. 10 A-B) however the variety of minerals seen in some samples (Fig. 10 C-D)
403 is likely the result of material from lower strata being eroded out and remineralised here. This
404 material is described here as mineralised musculature due to a consistent texture observed in
405 the grains resembling the striations of muscles.

406 **(Fig. 12 soft tissue impression photos)**

407

408 6.2 Taphonomy

409 The cause of death of the animal is unknown, as they are only partial remains without
410 any indicative features it is impossible to determine. However, given the condition of the
411 specimen it is probable the animal was dead prior to its arrival in the lagoon. *Susisuchus*
412 *anatoceps* has been described as a semi-aquatic crocodylian, probably inhabiting a fluvial
413 setting relatively near to the lagoon (Salisbury et al. 2003) where the animal died and was
414 subsequently washed into the lagoon. It is possible that the transportation and deposition of
415 the specimen could be sufficiently traumatic to result in the damage and disarticulation
416 observed in the dermal skeleton and axial skeleton. Given the relative good condition of the
417 specimen it is unlikely that the carcass was scavenged or predated upon. Whatever the cause
418 and mode of transport, the damaged carcass must have been held together by skin and sinew.
419 As the counter slab is missing it is unknown as to how complete the specimen could be.

420 Presumably the specimen arrived at the lagoon in a condition similar to that seen
421 fossilised. Anoxia in the lagoonal bottom waters would have inhibited macroscavengers, and

422 may also have delayed bacterial degradation. Despite some damage and disarticulation of the
423 specimen soft tissues did still remain on at least the left forelimb and on the flank of the torso.
424 The soft tissue of the torso, however, was damaged and torn from the skeletal component,
425 hanging from it as a sheet of flesh or skin or both. This could potentially have occurred when
426 the dermal skeleton disassociated from the specimen. The forelimbs of the animal, however,
427 were in good condition, fully articulated and with the musculature untouched in the left
428 forelimb at least. In order to preserve these soft tissues, it is necessary that the specimen
429 would have been buried rapidly after transportation. This is due to the rapid disarticulation
430 and decay crocodylians undergo if not prevented from floating (Syme and Salisbury, 2014).

431 Reduced decay in the anoxic bottom waters of the Cretaceous lagoon permitted the
432 mineralisation of soft tissues (Heimhofer and Martill, 2007). As the sediments lithified an
433 impression (external mould) of the torso integument was left in the rock, possibly with
434 mineralised tissues too, however if these were present that have since been eroded away. At
435 the same time the soft tissues of the left forelimb were mineralised, possibly as a result of
436 anaerobic, microbial activity, preserving the musculature and sequestering minerals and
437 elements present in the lagoon as available resources. During this time the slowly decaying
438 organism acted as a nucleus for silicification around the manus of the left forelimb and the
439 left hind limb.

440

441 **7. Discussion**

442 Presently two crocodylian species in two genera have been reported in the Crato
443 Formation: *Susisuchus anatoceps* (Salisbury et al., 2003) and *Araripesuchus* sp. (Frey and
444 Salisbury, 2007). As previously mentioned, the Crato Formation has not yielded many
445 crocodylians in the past, besides the specimen described here there are three other specimens

446 of *Susisuchus anatoceps* reported (Salisbury et al., 2003, Figueiredo and Kellner, 2009,
447 Figueiredo et al., 2011) and only one specimen of *Araripesuchus* sp. (Frey and Salisbury,
448 2007). This scarcity in specimens is likely a result of the animals avoiding the lagoon due to
449 their inferred lifestyles, *Susisuchus anatoceps* as a fluvial semi-aquatic animal and
450 *Araripesuchus* sp. as a terrestrial hunter or forager (Frey and Salisbury, 2007).

451 Despite the scarcity of crocodylian remains in the Crato formation soft tissues have
452 previously been reported in the holotype specimen of *Susisuchus anatoceps* (SMNK-PAL
453 3804) and could potentially be present in *Araripesuchus* sp. (SMNK-PAL 6404). SMNK-
454 PAL 3804 is described as having orange-brown stains, restricted to the forelimbs, the right
455 manus and cranium, which are considered to be the result of goethitic weathering of pyritised
456 soft tissues (Salisbury et al., 2003). SMNK-PAL 6404 however is noted by the authors as
457 having a partial outline of the belly region preserved as a dark stain which may be preserved
458 soft tissues.

459 Unlike either of these specimens, this specimen (UERJ-PMB R07) is preserved with
460 two different modes of soft tissue preservation and is far more extensive in the amount
461 preserved. The first mode of soft tissue preservation, the mould of the dorsolateral
462 integument of the skin (Fig. 12), is a typical form of preservation and is noted in other
463 specimens from the Crato Formation and other localities (Martill et al., 2007). The second
464 mode of soft tissue preservation, the mineralisation of the soft tissues around the right
465 forelimb (Fig. 6), proves far more enigmatic. This kind of mineralisation is not recognised in
466 any other specimen described from the Crato Formation and is believed to be the first account
467 of its occurrence.

468 The cause of this mineralisation is currently unknown but we hypothesise that it is
469 still likely a result of anaerobic bacterial decay in the anoxic bottom waters of the lagoon.

470 This resulted in minerals in the water, eroded from lower strata in the formation, being used
471 in the mineralisation process. No other fossils looked at from the Crato Formation appear to
472 demonstrate this mode of soft tissue preservation, as such it is considered a rare occurrence
473 for the formation suggesting that the conditions that generate this mineralisation were
474 similarly rare in the lagoon or that such conditions are not conducive to fossilisation. It is
475 important to further investigate the occurrence of this mode of preservation in the Crato
476 Formation and other formations to better understand the taphonomic pathway in effect.

477

478 **8. Conclusions**

479 UERJ-PMB R07 is considered here to be the fourth specimen of *Susisuchus* from the
480 Crato Formation diagnosed using features of the forelimb. The specimen is relatively intact
481 and provides new details on the anatomy and morphology of *Susisuchus*. This is the first
482 specimen of *Susisuchus* to be reported with hind limbs in association with diagnostic
483 material, the only other instance of a hind limb being described as a single, isolated limb
484 (Figueiredo and Kellner, 2009). This specimen also demonstrates exquisite soft tissue
485 preservation with the most extensive amount preserved in a crocodile from the Crato
486 Formation. It is preserved as both a mould of the dorsolateral integument of the torso and as
487 enigmatic mineralised soft tissues around the right forelimb. The mineralised material
488 represents a previously unseen type of preservation for the formation and has been examined
489 using light microscopy, UV imaging, scanning electron microscopy and energy dispersive X-
490 ray spectrometry. This has elucidated the composition and relationship of the material with
491 the specimen but its origin remains poorly understood.

492

493 **Acknowledgements**

494 The authors would like to thank Steven Vidovic for assistance with ultra-violet
495 imaging, Dr Tony Butcher for technical support and Mrs Elaine Dyer for assistance with
496 SEM and EDX analysis. Dr Paulo Brito (Rio de Janeiro) is warmly thanked for his help with
497 aspects of Brazilian Cretaceous stratigraphy. Dino Frey (Karlsruhe) is thanked for granting
498 access to the holotype of *Susisuchus* and a new specimen of *Araripesuchus*. Steve Salisbury
499 is warmly thanked for his very helpful refereeing of this paper.

500

501 **References**

502

503 Baéz, A.M., Moura, G.J.B., Gómez, R.O. 2009. Anurans from the Lower Cretaceous Crato
504 Formation of northeastern Brazil: implications for the early divergence of neobatrachians.
505 *Cretaceous Research* 30, 829–846.

506 Batten, D.J. 2007. Spores and pollen from the Crato Formation: biostratigraphic and
507 palaeoenvironmental implications. In: Martill, D.M., Bechly, G. and Loveridge, R.F. (eds.)
508 2007. *The Crato Fossil Beds of Brazil: Window into an Ancient World*. pp. 566-573. London:
509 Cambridge University Press.

510 Bechly, G. 2007. Introduction: Insects of the Crato Formation. In: Martill, D.M., Bechly, G.
511 and Loveridge, R.F. (eds). *The Crato Fossil Beds of Brazil: Window into an Ancient World*.
512 142-148. London: Cambridge University Press.

513 Benton, M.J. and Clark, J.M. 1988. Archosaur phylogeny and the relationships of the
514 Crocodylia. In: Benton, M.J. (ed.), *The Phylogeny and Classification of Tetrapods*, vol. 1:
515 *Amphibians, Reptiles, Birds Systematics Association Special Volume 35A*. Oxford:
516 Clarendon press.

- 517 Beurlen, K.A. 1962. A geologia da Chapada do Araripe. Anais da Academia Brasileira de
518 Ciencias 34, 365-370.
- 519 Brito, P.M. 2007. The Crato Formation fish fauna. In: Martill, D.M., Bechly, G. and
520 Loveridge, R.F. (eds.). The Crato Fossil Beds of Brazil: Window into an Ancient World. 429-
521 443. London: Cambridge University Press.
- 522 Dunlop, J.A., Menon, F. and Selden, P.A. 2007. Arachnida: spiders, scorpions and allies. In:
523 Martill, D.M., Bechly, G. and Loveridge, R.F. (eds.). The Crato Fossil Beds of Brazil:
524 Window into an Ancient World. 103-132. London: Cambridge University Press.
- 525 Fielding, S., Martill, D.M. and Naish, D. 2005. Solnhofen-style soft-tissue preservation in a
526 new species of turtle from the Crato Formation (Early Cretaceous, Aptian) of north-east
527 Brazil. Palaeontology 48, 1301-1310.
- 528 Figueiredo, R.G. and Kellner, A.W.A. 2009. A new crocodylomorph specimen from the
529 Araripe Basin (Crato Member, Santana Formation), northeastern Brazil. Paläontologie
530 Zeitschrift 83, 323-331.
- 531 Figueiredo, R.G., Moreira, J.K.R., Saraiva, A.Á.F. and Kellner, A.W.A. 2011. Description of
532 a new specimen of *Susisuchus anatoceps* (Crocodylomorpha: Mesoeucrocodylia) from the
533 Crato Formation (Santana Group) with comments on Neosuchia. Zoological Journal of the
534 Linnean Society 163, S273-S288.
- 535 Fortier, D.C. and Schultz, C.L. 2009. A new neosuchian crocodylomorph (Crocodyliformes,
536 Mesoeucrocodylia) from the Early Cretaceous of North-East Brazil. Palaeontology 52, 991-
537 1007.
- 538 Frey, E., Martill, D.M., Buchy, M.-C. 2003a. A new species of tapejarid pterosaur with soft-
539 tissue head crest. The Geological Society, London, Special Publications 217, 65-72.

- 540 Frey, E., Tischlinger, H., Buchy, M.-C., Martill, D.M. 2003b. New specimens of Pterosauria
541 (Reptilia) with soft parts with implications for pterosaurian anatomy and locomotion. The
542 Geological Society, London, Special Publications 217, 233-266
- 543 Frey, E. and Salisbury, S.W. 2007. Crocodylians of the Crato Formation: evidence for
544 enigmatic species. In: Martill, D.M., Bechly, G. and Loveridge, R.F. (eds.) 2007. The Crato
545 Fossil Beds of Brazil: Window into an Ancient World. 463-474. London: Cambridge
546 University Press.
- 547 Hay, O.P., 1930. Second Bibliography and Catalogue of the Fossil Vertebrata of North
548 America, Vol. 2. Carnegie Institution of Washington, Washington DC 2, 1094 pp.
- 549 Heimhofer, U., Martill D.M. 2007. The sedimentology and depositional environment of the
550 Crato Formation. In: Martill, D.M., Bechly, G. and Loveridge, R.F. (eds.). The Crato Fossil
551 Beds of Brazil: Window into an Ancient World. pp. 44-62. London: Cambridge University
552 Press.
- 553 Kellner, A.W.A. 1996. Description of new material of Tapejaridae and Anhangueridae
554 (Pterosauria, Pterodactyloidea) and discussion of pterosaur phylogeny. PhD thesis, Columbia
555 University.
- 556 Kellner, A.W.A., Campos, D.A. 2007. Short note on the ingroup relationships of the
557 Tapejaridae (Pterosauria, Pterodactyloidea). Boletim do Museu Nacional
558 Nova Série, Geologia 75, 1-14.
- 559 Martill, D.M. 2007. Lizards of the Crato Formation. In: Martill, D.M., Bechly, G. and
560 Loveridge, R.F. (eds). The Crato Fossil Beds of Brazil: Window into an Ancient World. 463-
561 474. London: Cambridge University Press.

- 562 Martill, D.M., Bechly, G. and Loveridge, R.F. (eds) 2007. The Crato Fossil Beds of Brazil:
563 Window into an Ancient World. London: Cambridge University Press.
- 564 Martill, D.M. and Heimhofer, U. 2007. Stratigraphy of the Crato Formation. In: Martill,
565 D.M., Bechly, G. and Loveridge, R.F. (eds). The Crato Fossil Beds of Brazil: Window into an
566 Ancient World. pp. 25-43. London: Cambridge University Press.
- 567 Martill, D.M., Tischlinger, H. and Longrich, N.R. 2015. A four-legged snake from the Early
568 Cretaceous of Gondwana. *Science*. 6246, 416-419
- 569 Mohr, B.A.R., Bernardes-de-Oliveira, M.E.C. and Loveridge, R. F. 2007. The macrophyte
570 flora of the Crato Formation. In: Martill, D.M., Bechly, G. and Loveridge, R.F. (eds). The
571 Crato Fossil Beds of Brazil: Window into an Ancient World. 463-474. London: Cambridge
572 University Press.
- 573 Naish, D. 2007. Turtles of the Crato Formation. In: Martill, D.M., Bechly, G. and Loveridge,
574 R.F. (eds.) 2007. The Crato Fossil Beds of Brazil: Window into an Ancient World. 452-457.
575 London: Cambridge University Press.
- 576 Sayão, J.M., Bantim, R.A.M., Andrade, R.C.L.P., Lima, F.J., Saraiva, A.A.F., Figueiredo,
577 R.G. and Kellner, A.W.A. 2016. Paleohistology of *Susisuchus anatoceps* (Crocodylomorpha,
578 Neosuchia): Comments on Growth Strategies and Lifestyle. PLoS ONE 11(5), e0155297
- 579 Salisbury, S.W., Frey, E., Martill, D.M. and Buchy, M.-C. 2003. A new crocodylian from the
580 Lower Cretaceous Crato Formation of north-eastern Brazil. *Palaeontographica Abteilung A*.
581 270, 3-47
- 582 Schweigert, G., Martill, D.M. and Williams, M. 2007. Crustacea of the Crato Formation. In:
583 Martill, D.M., Bechly, G. and Loveridge, R.F. (eds.) 2007. The Crato Fossil Beds of Brazil:
584 Window into an Ancient World. 133-141. London: Cambridge University Press.

585 Syme, C.E., Salisbury, S.W. 2014. Patterns of aquatic decay and disarticulation in juvenile
586 Indo-Pacific crocodiles (*Crocodylus porosus*), and implications for the taphonomic
587 interpretation of fossil crocodyliform material. *Palaeogeography, Palaeoclimatology,*
588 *Palaeoecology* 412, 108–123.

589 Unwin, D. M. and Martill, D.M. 2007. Pterosaurs of the Crato Formation. In: Martill, D.M.,
590 Bechly, G. and Loveridge, R.F. (eds.) 2007. *The Crato Fossil Beds of Brazil: Window into an*
591 *Ancient World*. 463-474. London: Cambridge University Press.

592 Whetstone, K.N., Whybrow, P.J. 1983. A “cursorial” crocodylian from the Triassic of
593 Lesotho (Basutoland), southern Africa. *Occasional Papers of the Museum of Natural History,*
594 *The University of Kansas* 106, 1-37.

595

596 **FIGURE CAPTIONS**

597

598 **Fig. 1.** Locality map of the aerial extent of the Araripe Basin of North East Brazil. The new
599 specimen was collected from a quarry between Crato and Nova Olinda.

600

601 **Fig. 2.** A stratigraphic log of the Crato Formation as exposed approximately 4 km south of
602 Nova Olinda, Ceará, Brazil. The exposure comprises the lower three Crato Formation
603 member: the Nova Olinda Member, a homogenous laminated limestone; the Caldas Member,
604 heterolithic strata of mudstone, silts and siltstone; and the Jamacaru Member, a sequence of
605 alternating laminated limestones and mudstone. (Heimhofer et al., 2010)

606

607 **Fig. 3.** The new specimen of crocodylomorph UERJ-PMB R07, here referred to *Susisuchus*
608 sp. (Scale bar: 10 mm).

609

610 **Fig. 4.** A schematic representation of UERJ-PMB R07; *Susisuchus* sp. (Scale bar: 10 mm).

611 *Abbreviations used: Adhes.:* Adhesive. *Ost.:* Osteoderm. *Fem.:* Femur. *Fib.:* Fibula. *Hum.:*

612 Humerus. *M. Tars.:* Metatarsals. *Neur. Can.:* Neural Canal. *Pec. Girdle:* Pectoral Girdle.

613 *Pub.:* Pubis *Tars.:* Tarsals. *Trans. Proc.:* Transverse Process. *Vert.:* Vertebra. *L.:* Left. *R.:*

614 Right.

615

616 **Fig. 5. A:** Thoracic and disarticulated paired lumbar vertebrae of UERJ-PMB R07 preserved
617 in ventral view. **B:** A schematic diagram of the vertebral elements of UERJ-PMB R07. (Scale

618 bar: 10 mm).

619

620 **Fig. 6.** The forelimbs of UERJ-PMB R07. **A,** The right forelimb surrounded by preserved soft

621 tissues with a fragment of the pectoral girdle covering the proximal humerus. **B,** A schematic

622 diagram of the right forelimb. **C,** The left forelimb with an isolated, disarticulated osteoderm.

623 **D,** A schematic diagram of the left forelimb. (Scale bar: 10 mm).

624

625 **Fig. 7.** The hind limbs of UERJ-PMB R07. **A,** The left hind limb. Elements of the pelvic

626 girdle are preserved around the proximal femur and soft tissue mineralisation is noted around

627 the femur. **B,** A schematic diagram of the left hind limb. **C,** The right hind limb with

628 surrounding silicification. **D,** A schematic diagram of the right hind limb. (Scale bar: 10 mm).

629

630 **Fig. 8. A,** The mineralised soft tissue of the right forelimb extending beneath the bone, as

631 exposed beneath the broken humerus. (Scale bar: 5 mm) **B:** Individual grains in the

632 mineralised soft tissue growing into the surrounding mineral matrix. (Scale bar: 2 mm).

633

634 **Fig. 9.** SEM images of the soft tissue material surrounding the right forelimb. **A-C**, Grains of
635 mineralised material showing a rounded, irregular morphology. (Scale bar: **A**, 200 μm **B**, 600
636 μm **C**, 600 μm) **D**, Detail of the crust of the grains showing the porous surface. (Scale bar:
637 200 μm) **E-F**, Orthogenic calcite growths observed on grains, typically on broken surfaces.
638 (**E**, Scale bar: 60 μm **F**, 100 μm).

639

640 **Fig. 10. A-B**, Results of EDX analysis of the mineralised material surrounding the right
641 forelimb showing the primary composition of grains as calcium carbonate and iron oxides. **C-**
642 **D**, Results of EDX analysis demonstrating the variety in elemental composition that occur
643 less frequently in the mineralised material surrounding the left forelimb, typically found on
644 the surface of grains.

645

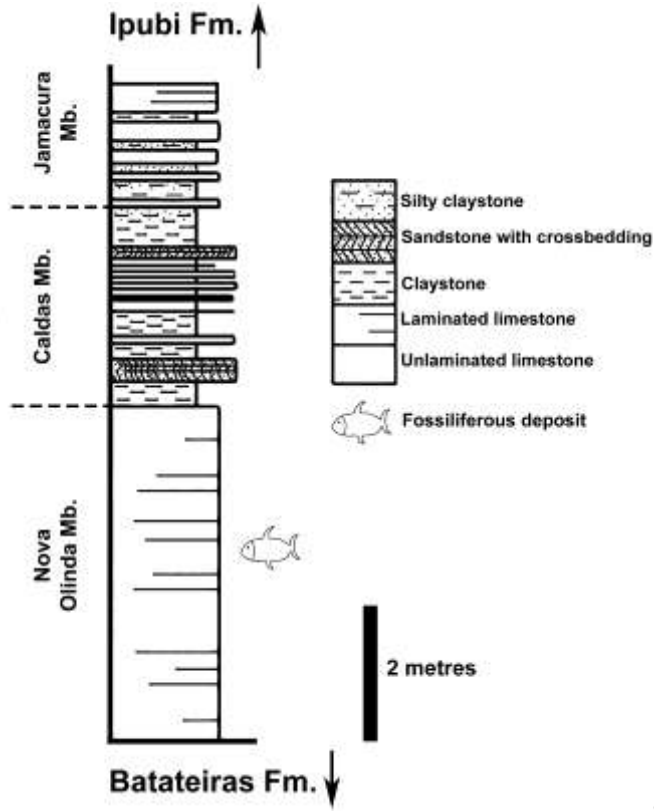
646 **Fig. 11.** UV imaging using a green filter. **A**, The right hind limb, with surrounding possible
647 soft tissue and adjacent thoracic vertebrae. (Scale bar: 10 mm) **B**, The right forelimb,
648 surrounding soft tissue and silicified sediment. (Scale bar: 10 mm).

649

650 **Fig. 12. A**, The soft tissue impression of the scales of the dorsolateral surface of the trunk.
651 (Scale bar: 10 mm) **B**, The soft tissue impression of the trunk scales under high angle lighting
652 highlighting its topography. (Scale bar: 10 mm).

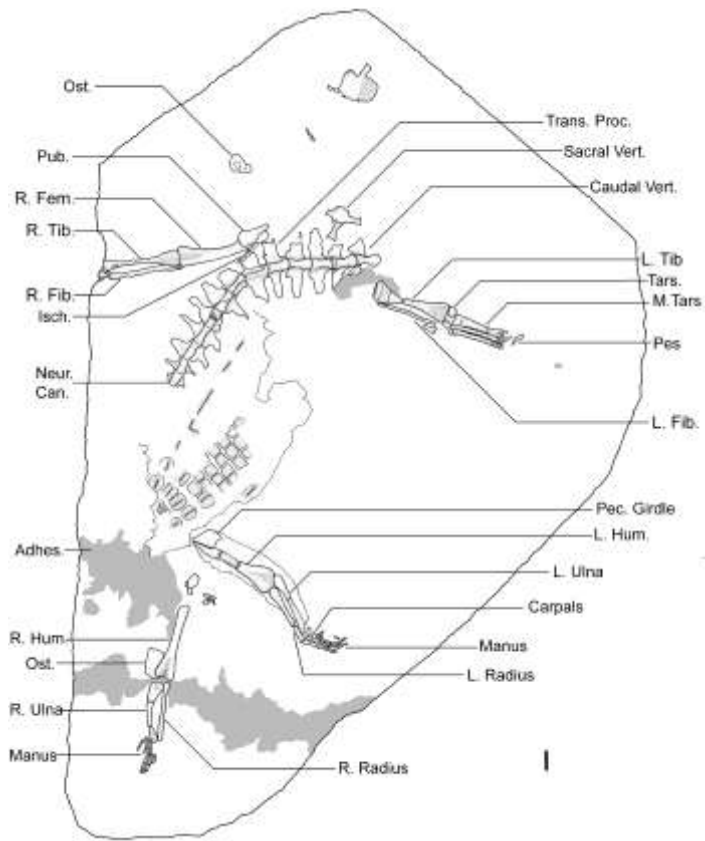
653

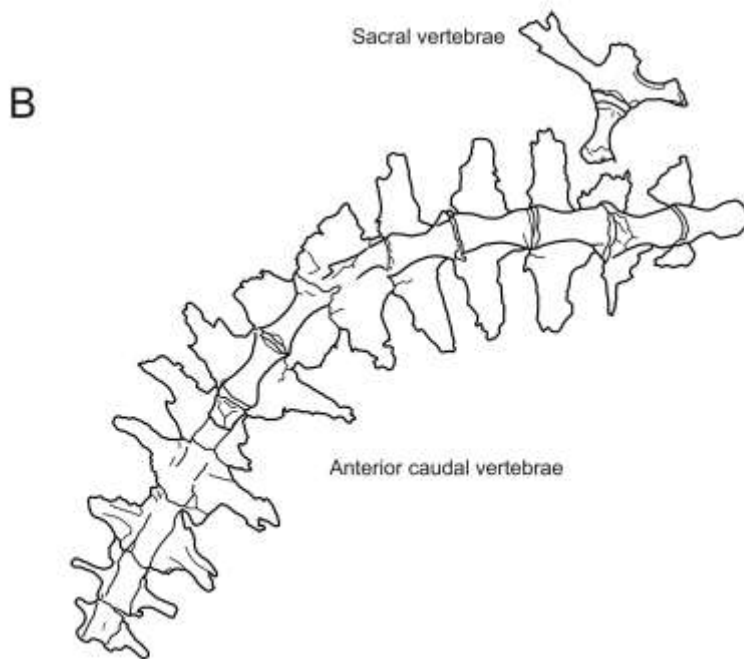


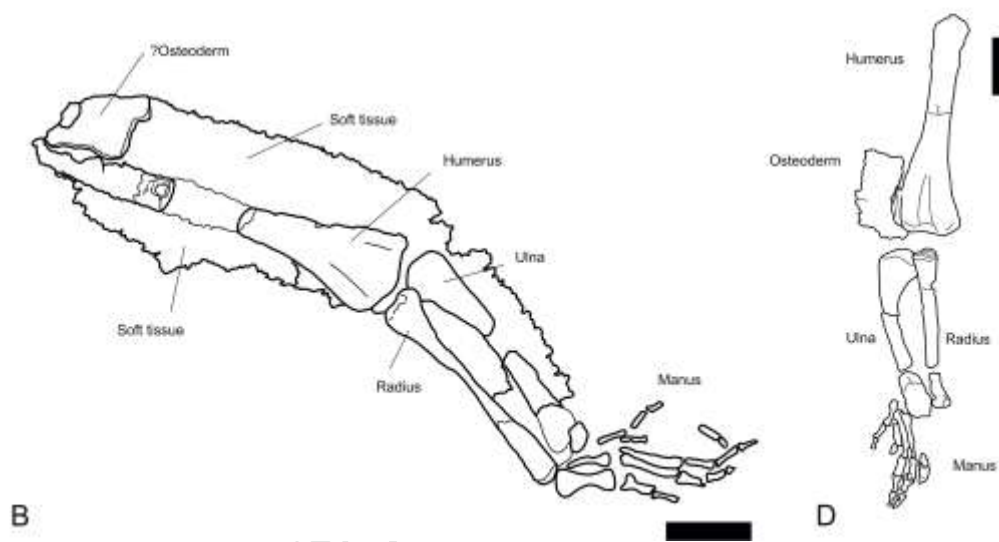


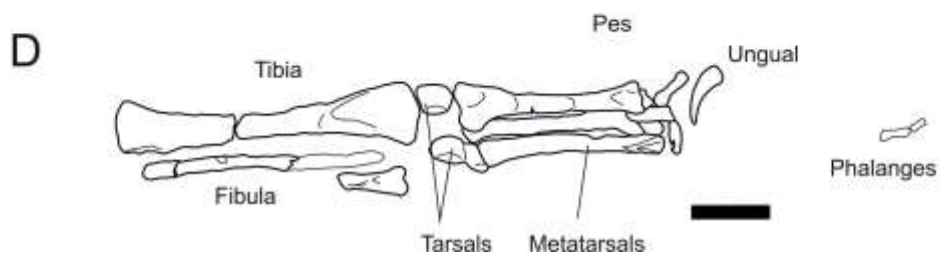
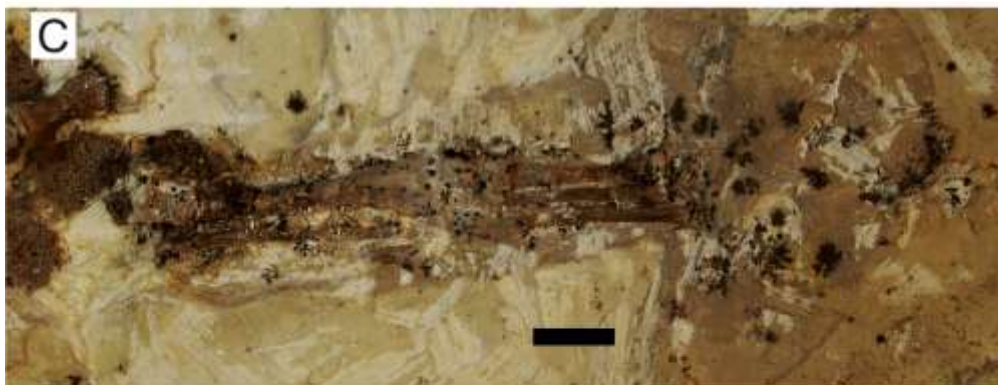
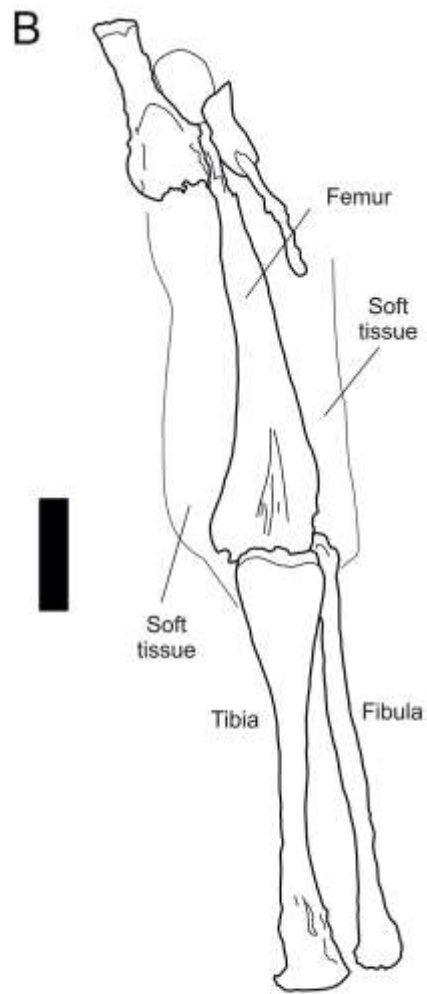


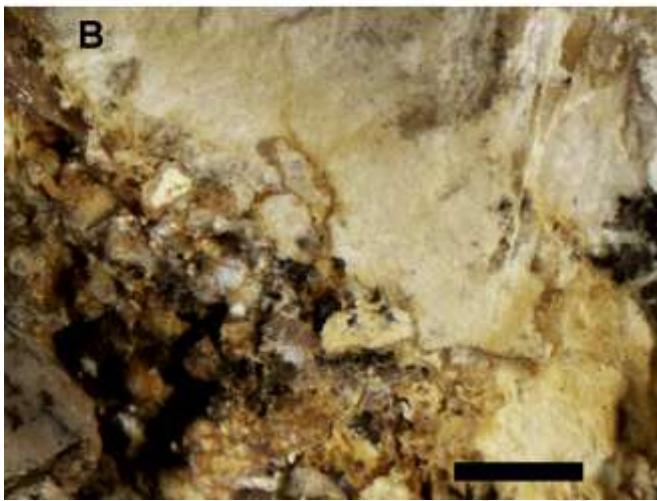
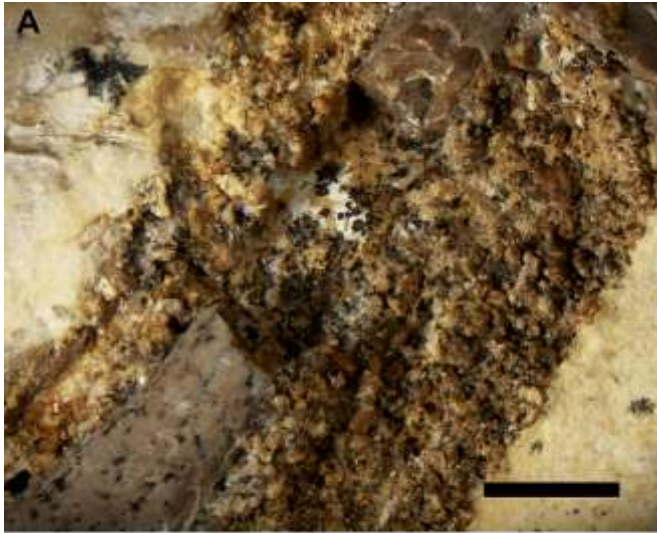
ACCEPTED MANUSCRIPT



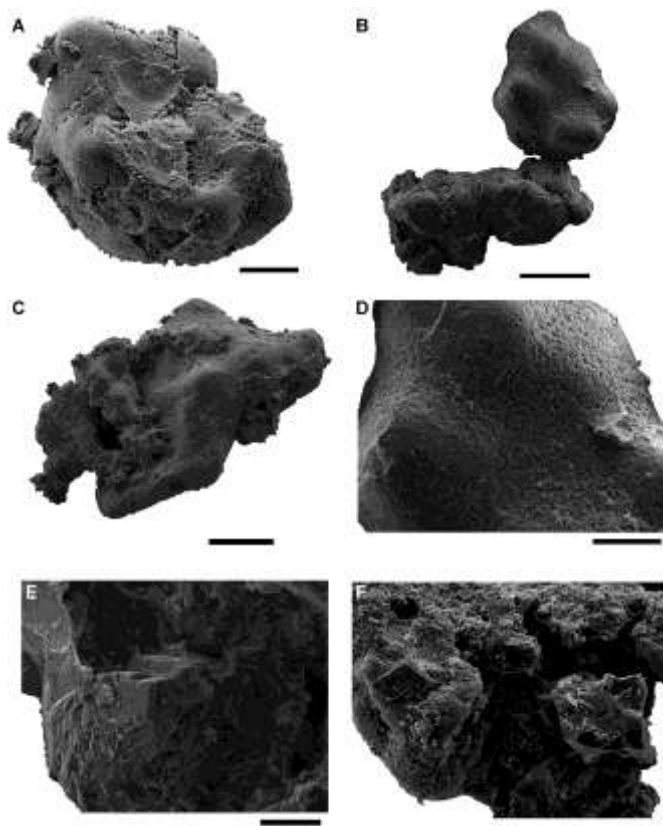


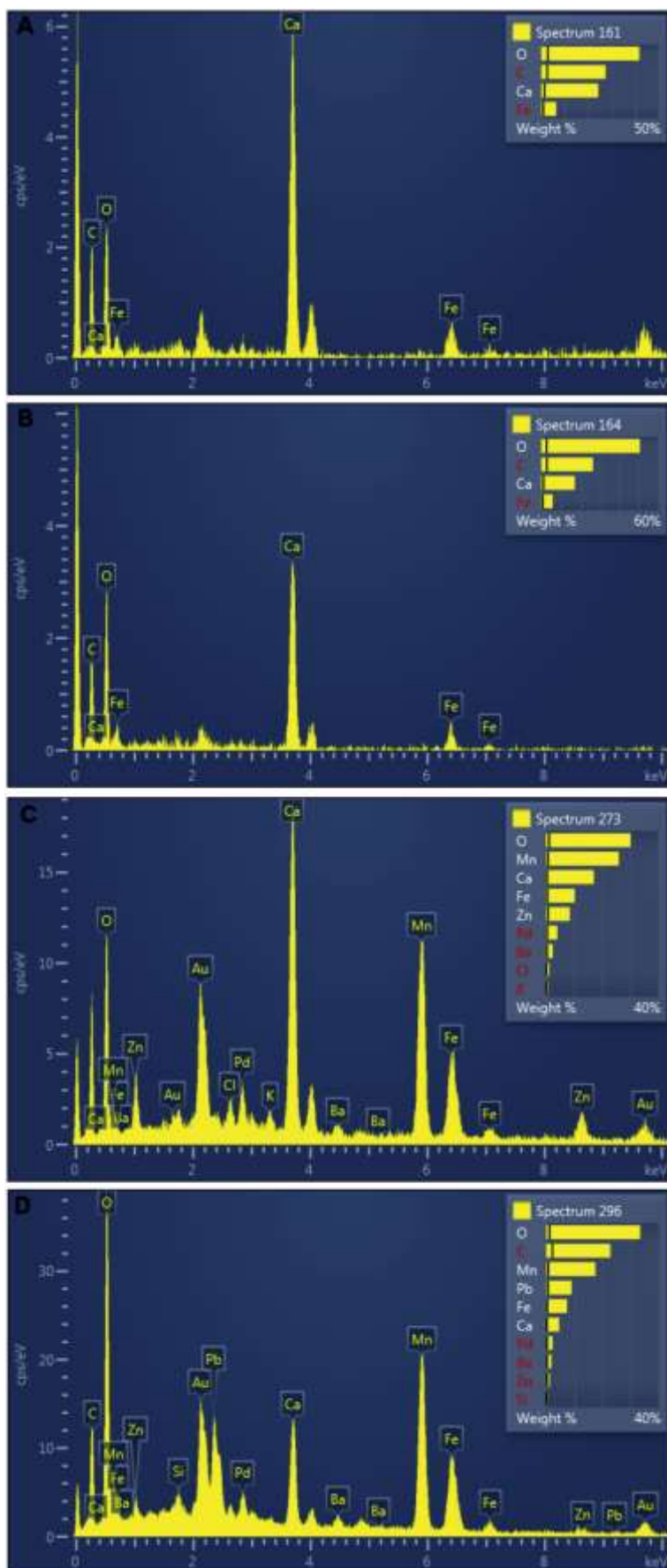






ACCEPTED MANUSCRIPT







ACCEPTED MANUSCRIPT

